

Spectral Selective High Emissivity Pattern for Applications in near Infrared

Enrique Carretero, Rafael Alonso and Cristina Pelayo

Department of Applied Physics, University of Zaragoza, C/Pedro Cerbuna, 12, 50009 Zaragoza, Spain

Keywords: Spectral Selective, Emissivity, Thin Films, Sputtering.

Abstract: In this work, we develop some high emissivity patterns for the near infrared range, between 1200 and 2500nm. These patterns were made by means of the magnetron sputtering technique, and they achieve their functionality by using the optical interference phenomenon so that their superficial reflectance is diminished. This is how we manage to produce surfaces that have a very low reflectance and high spectral emissivity in the abovementioned range. Such patterns can be used for the calibration of temperature-measuring systems based on photodiodes detecting near infrared radiation.

1 INTRODUCTION

It is well known that all bodies emit radiation, as the black body theory describes. The total hemispherical spectral emissive power or radiance of a surface (DeWitt and Nutter, 1988; Howell et al., 2015), namely, $E_{\lambda}(\lambda, T)$, is the power density distribution emitted into the hemispherical solid per unit of surface area whose dependence is provided by the following equation:

$$E_{\lambda}(\lambda, T) = \frac{2\pi hc^2}{\lambda^5 (e^{hc/\lambda kT} - 1)} \quad (1)$$

where T is the absolute temperature, λ is the wavelength of the radiation, h is the Planck constant, c is the speed of light in vacuum and k is the Boltzmann constant. But real bodies do not emit radiation in the same way as a black body would do, because they are not really "black". The concept of "emissivity" is introduced to take this into account. The emissivity of an object is determined by its absorption, so it can be measured with a spectrophotometer, using the following expression:

$$\varepsilon(\lambda) = 1 - R(\lambda) - T(\lambda) \quad (2)$$

where $\varepsilon(\lambda)$ is the spectral emissivity of the object, $R(\lambda)$ is its spectral reflectance and $T(\lambda)$ is its spectral transmittance. In this way, the total hemispherical spectral emissive power or radiance of a real surface is:

$$E_{\lambda}(\lambda, T) = \varepsilon(\lambda) \frac{2\pi hc^2}{\lambda^5 (e^{hc/\lambda kT} - 1)} \quad (3)$$

Emissivity is very important for a lot of applications, for instance, in the field of concentrated solar power. The receiver tubes where solar radiation must be concentrated on need to be highly absorbent, that is, they need to have a high emissivity in the spectral range where the sun emits its maximum radiation (black body radiation at 5700K), between 300 and 2500nm (Setien-Fernandez et al., 2013). At the same time, these tubes must keep at a minimum the losses due to emitted radiation when heated to 673K, so they must have a low emissivity in the spectrum range of a black body at 673K, between 2.5 and 30 μm . In order to fulfil these requirements, selective coatings are deposited by PVD (Physical Vapour Deposition) techniques (Cao et al., 2015; Céspedes et al., 2014; Hernandez-Pinilla et al., 2016; H.J.Gläser, 2000).

Nowadays, the improved performance and lowered prices of InGaAs PIN photodiodes has allowed its use for small signal detection in near infrared for domestic appliances, temperature measurement in cooking vessels from cooktops being one example of this. This system is based on the measurement of the black body radiation emitted by a pot when cooking at temperatures between 100 and 200°C (Imaz et al., 2014; Lasobras et al., 2014). The photodiode is located inside the cooktop, under the ceramic glass surface, so light detection must be carried out in a wavelength range where the ceramic glass is transparent. Such requirement rules out other

options measuring in wavelength ranges above $3\mu\text{m}$, although pots and pans in the abovementioned cooking temperature range emit most of the radiation above $3\mu\text{m}$. InGaAs photodiodes detect radiation between 600 and 2500nm. A surface heated to 100°C emits very little power in this wavelength range, but this type of photodiodes is sensitive enough to measure it.

One important issue with these detectors is its calibration. They need to be calibrated with very low emissive patterns and also with very high emissive patterns. Low emissive patterns are very easy to produce, because there is a great number of metals which are low emissive in near infrared, as gold. On the other hand, it's easy to find a high emissive surface with values around $\varepsilon=0.90$ in the detection range of InGaAs PIN photodiodes, such as "burnt-out" surfaces, but we have been able to produce a pattern which has a higher emissivity ($\varepsilon>0.97$) than traditional surfaces in this detection range. Such patterns permit us to obtain a greater signal in the temperature sensor of a cooktop.

Highly emissive patterns were produced by means of the magnetron sputtering technique. These patterns can be obtained by combining metallic and dielectric layers (Sergeant et al., 2009). A coating was deposited comprised of 4 layers, using both an absorbent metallic material (Stainless Steel 316) and a transparent dielectric material (SiAlN_x) in a way that the coating results opaque ($T=0$) and has a minimal superficial reflectance between 1200 and 2500nm, using interferential coatings.

2 MATERIAL AND METHODS

Spectral Selective High Emissivity Patterns were deposited in a semi-industrial high vacuum magnetron sputtering system by the DC pulsed technique using rectangular targets with dimensions $600\times 100\text{mm}$ and 12mm thick. Substrates were ceramic glass pieces of $100\times 100\text{mm}$ and 4mm thick. Ceramic glass has low thermal expansion coefficient which makes it resistant to high temperature gradients without breaking. Substrates were cleaned with a detergent solution (ACEDET 5509) and finally rinsed with distilled water. A Stainless Steel disc was also used to simulate a rough metallic surface.

Thin films were grown with a base pressure of $2.0\cdot 10^{-6}$ mbar and working pressure in the range of 10^{-3} mbar. Ar and O_2 (both 99.99%) flows were introduced into the process chamber and controlled via mass flow controllers. The substrate was maintained at room temperature during deposition.

Thin films of Stainless Steel (Sst) were deposited from a Sst 316 target (99.99% pure). Applied power was 2000W, equivalent to a power density of $3.33\text{W}/\text{cm}^2$. The Ar flow was fixed at 200sccm, equivalent to a pressure of $1.5\cdot 10^{-3}$ mbar in our deposition system. Thin films of SiAlN_x were deposited by reactive sputtering from a Si-Al target (90% Si and 10% Al, 99.99% pure). Applied power was 2500W, equivalent to a power density of $4.17\text{W}/\text{cm}^2$. The Ar flow was fixed at 100sccm and the N_2 flow at 100sccm.

Spectrophotometric measurements were performed with a home-made spectrophotometer (designed and built by some of the authors) in the near-infrared region of the electromagnetic spectrum, between 1100nm and 2500nm with 50nm intervals, at an angle of incidence of 8° . The specular reflectance of the patterns deposited over smooth surfaces was measured without an integrating sphere, because the low roughness of the substrate minimizes the scattered component to negligible values and because the specular measurements are more precise. For patterns deposited over a rough surface, reflectance measurements were carried out through an integrating sphere. Finally, a transmittance measurement was taken to verify the low transmittance of the patterns.

3 RESULTS AND DISCUSSION

There are diverse types of InGaAs photodiodes having different sensitive ranges. The most common ones are those capable of detection radiation between 600 and 1700nm, but there are extended sensitivity models which can detect radiation between 800 and 2600nm. On the other hand, temperature sensors must be calibrated between 100 and 250°C , and in this temperature range the black body radiation below 1200nm is negligible. So the objective of this work is to minimize reflectance in the range between 1200 and 2500nm. For this purpose, we designed an interference multilayer comprised of 4 layers, fig.1:

A first "thick" metallic layer (over 200nm) directly deposited on the substrate. This layer has a double functionality: for transparent substrates, this layer has a high optical absorption, so the pattern can be opaque ($T=0$), and furthermore, it will act as a basic layer to calculate the interferential coating which minimizes reflectance between 1200 and 2500nm.

The thicknesses of the three subsequent layers must be adjusted very precisely, because they

determine the reflectance of the pattern. For this purpose, the coating was simulated with the aid of existing formalisms for the calculation of the optical properties of interferential coatings (J. A. Dobrowolski, 1995; Macleod, 2010; Thelen, 1989). Values minimizing reflectance as required are shown in table 1.

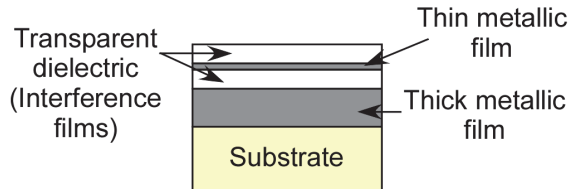


Figure 1: Multilayer structure of high emissivity patterns.

Table 1: Multilayer structure and layer thicknesses of produced patterns.

Material	Thickness (nm)
Substrate	
Sst	>200
SiAlN _x	186
Sst	13
SiAlN _x	204

Thus, we proceeded with the experimental making of the patterns, both on ceramic glass and on metallic discs, as depicted in Fig.2. So two patterns were made: a specular pattern and a non-specular one, the last one owing its feature to the roughness of the substrate surface. These patterns visually appear as purple coloured, because interferential coatings usually produce striking colours. The fact that they are (almost) black bodies in the 1200-2500nm range is remarkable, considering this is not true for the visible part of the spectrum, as they indeed have a high reflectance at some particular wavelengths.

Figure 3 shows the reflectance curves of the two produced patterns. In both cases we find similar values of reflectance in spite of the differences over surface texture of both substrates. Additionally, measured values satisfactorily agree with simulated values. On behalf of these results and knowing the sensibility of the photodiodes provided by the manufacturer, which in this particular case is Teledyne Judson Technologies LLC, as we have used models J22-18I-R01M and J2318I-R01M-2.6 (detecting respectively up to 1700 and 2600nm), we can calculate the integrated apparent emissivity of our patterns with this expression:

$$\epsilon_{1700}(T) = \frac{\int_0^{\infty} S_{1700}(\lambda) \cdot E(T, \lambda) \cdot (1 - R(\lambda)) d\lambda}{\int_0^{\infty} S(\lambda) \cdot E(T, \lambda) d\lambda} \quad (4)$$

Where S is the sensitivity of the J22-18I-R01M photodiode, R is the spectral reflectance of the pattern, ϵ is the integrated apparent emissivity at the temperature T of the pattern as calculated for the photodiode which detects up to 1700nm. This last magnitude has a value of $\epsilon_{1700}(473K)=0.987$ for a temperature of 473K.



Figure 2: Images of the produced patterns on ceramic glass (top) and on a rough metallic disc (bottom).

We can repeat this procedure for the extended-range photodiode that detects up to 2600nm, modifying only the value of $S_{1700}(\lambda)$ for $S_{2600}(\lambda)$ in expression (4), and we obtain an integrated apparent emissivity of $\epsilon_{2600}(473K)=0.976$ Finally, we were able to verify that our patterns produced the greatest measured signals over all surfaces that were measured with the temperature sensor (Imaz et al., 2014; Lasobras et al., 2014).

One must keep in mind that the integrated apparent emissivity is a magnitude taking into account the spectral width between 1200 and 2600nm. Concerning spectral emissivity, values as high as $\epsilon(1850\text{nm})=0.994$ were reached. Nevertheless, if the final aim of the pattern was to maximize emissivity at a particular wavelength (instead of a wide range), it could be possible to obtain values closer to 1.

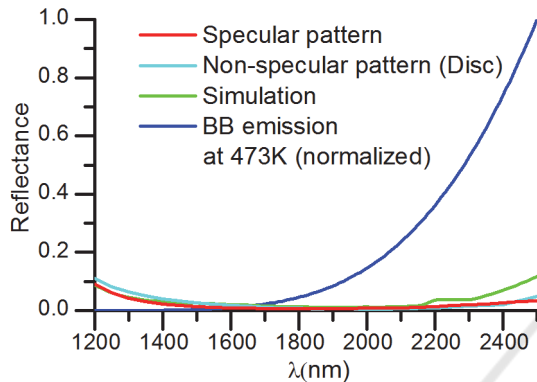


Figure 3: Reflectance curves measured and simulated for the highly emissive produced patterns, and normalized black body emission at 473K.

One very significant issue is the tolerance in the thickness of the deposited layers, because any variation in these thicknesses can affect the reflection spectrum of the pattern. Figure 4 shows the changes in reflection spectra for coatings in which some of its layers have a thickness deviated from the values given in Table 1. One can appreciate in this figure how an increment in the thickness of the outer layer increases reflectance in the 1200-1800nm range and decreases it in the 2100-2500nm range. On the other hand, a 10% increment in both dielectric layers shifts the low reflectance zone towards higher wavelengths, whereas a 10% increment in all the coating layers produces a slight displacement and narrowing of the low reflectance zone. If the thin metallic film has a 30% thinner thickness, the wide part of the spectrum with low reflectance disappears and two reflectance minimums appear at 1250 and 2300nm. If that same film has a 30% thicker thickness, the low reflectance zone is narrowed but very low reflectance values can be achieved at a specific wavelength (1780nm for the studied case).

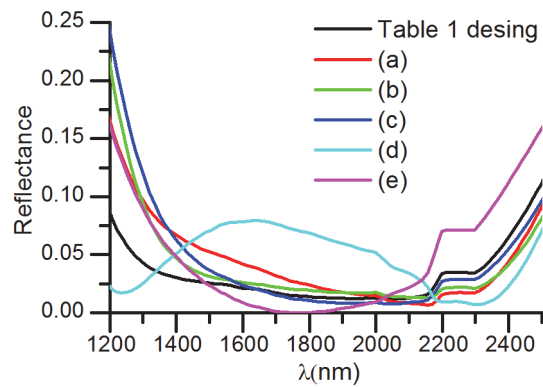


Figure 4: Simulated reflectance spectra for coatings with different thicknesses: multilayer structure as described in Table 1 (black line), (a) Outer transparent dielectric layer with a 10% thicker thickness than in Table 1, (b) both dielectric layers with a 10% thicker thickness, (c) All layers with a 10% thicker thickness, (d) Thin metallic film with a 30% thinner thickness, (e) Thin metallic film with a 30% thicker thickness.

So it can be concluded that layer thicknesses must be adjusted with a tolerance lower than 10% and preferably lower than 3%. Nevertheless, coating adjustment is an iterative process where a coating is deposited with thickness values near those exposed in the table, then the reflectance of the coating is measured and the experimentally obtained results are adjusted by means of a simulation software in such a way that we can know which thicknesses must be modified for a better adjustment of optical properties. In this way, these results can be reproduced in other deposition systems, although small further tuning of thicknesses might be required.

It is remarkable that this kind of patterns can be produced using different materials. Other dielectric materials such as oxides and nitrides (SnO_2 , Al_2O_3 ...) can be used, although they may require thicknesses to be recalculated because of their different index of refraction. SSt can also be replaced by other metals commonly employed for the fabrication of selective coatings in the solar energy field, such as Mo, W...

4 CONCLUSIONS

Highly emissive patterns can be used to calibrate temperature sensors based on infrared radiation detection. We have made two highly emissive patterns in the 1200-2500nm range, one of them being specular and the other diffuse on a rough

surface, and both reaching values over 0.97. Moreover, we have proven the feasibility of reaching spectral emissivities over 0.99 at particular wavelengths, by means of interferential multilayer deposition. These patterns were used to calibrate a temperature sensor. Finally, a good agreement between simulated and measured values of reflectance has been verified for these coatings.

ACKNOWLEDGEMENTS

We thank Carmen Cosculluela for her valuable help. This work was partly supported by the Spanish MINECO under grant RTC-2014-1847-6, in part by the Diputación General de Aragón / Fondo Social Europeo through the funding for the Photonics Technologies Group (GTF), in part by the Diputación General de Aragón under FPI programme B143/12 and in part by the BSH Home Appliances Group.

REFERENCES

- Cao, F., Kraemer, D., Sun, T., Lan, Y., Chen, G., Ren, Z., 2015. *Enhanced Thermal Stability of W-Ni-Al₂O₃ Cermet-Based Spectrally Selective Solar Absorbers with Tungsten Infrared Reflectors*. *Adv. Energy Mater.* 5, 1401042. doi:10.1002/aenm.201401042.
- Céspedes, E., Wirz, M., Sánchez-García, J.A., Alvarez-Fraga, L., Escobar-Galindo, R., Prieto, C., 2014. *Novel Mo-Si₃N₄ based selective coating for high temperature concentrating solar power applications*. *Sol. Energy Mater. Sol. Cells* 122, 217–225. doi:10.1016/j.solmat.2013.12.005.
- DeWitt, D.P., Nutter, G.D., 1988. *Theory and Practice of Radiation Thermometry*. John Wiley & Sons.
- Hernandez-Pinilla, D., Rodriguez-Palomo, A., Alvarez-Fraga, L., Cespedes, E., Prieto, J.E., Munoz-Martin, A., Prieto, C., 2016. *MoSi₂-Si₃N₄ absorber for high temperature solar selective coating*. *Sol. Energy Mater. Sol. Cells* 152, 141–146. doi:10.1016/j.solmat.2016.04.001.
- H.J.Gläser, 2000. *Large Area Coating*. Von Ardenne Anlagentechnik GmbH, Dresden.
- Howell, J.R., Menguc, M.P., Siegel, R., 2015. *Thermal Radiation Heat Transfer*, 6th Edition. CRC Press.
- Imaz, E., Alonso, R., Heras, C., Salinas, I., Carretero, E., Carretero, C., 2014. *Infrared thermometry system for temperature measurement in induction heating appliances*. *IEEE Trans. Ind. Electron.* 61, 2622–2630. doi:10.1109/TIE.2013.2281166.
- J. A. Dobrowolski, 1995. *Optical properties of films and coatings*, in: *Handbook of Optics*. McGraw-Hill.
- Lasobras, J., Alonso, R., Carretero, C., Carretero, E., Imaz, E., 2014. *Infrared sensor-based temperature control for domestic induction cooktops*. *Sens. Switz.* 14, 5278–5295. doi:10.3390/s140305278.
- Macleod, H.A., 2010. *Thin-Film Optical Filters*, Fourth Edition. CRC Press.
- Sergeant, N.P., Pincon, O., Agrawal, M., Peumans, P., 2009. *Design of wide-angle solar-selective absorbers using aperiodic metal-dielectric stacks*. *Opt. Express* 17, 22800–22812.
- Setien-Fernandez, I., Echaniz, T., Gonzalez-Fernandez, L., Perez-Saez, R.B., Cespedes, E., Sanchez-Garcia, J.A., Alvarez-Fraga, L., Escobar Galindo, R., Albella, J.M., Prieto, C., Tello, M.J., 2013. *First spectral emissivity study of a solar selective coating in the 150-600 degrees C temperature range*. *Sol. Energy Mater. Sol. Cells* 117, 390–395. doi:10.1016/j.solmat.2013.07.002.
- Thelen, A., 1989. *Design of Optical Interference Coatings*. McGraw-Hill.